Am J Physiol Renal Physiol 298: F589–F600, 2010.
First published December 23, 2009; doi:10.1152/ajprenal.00628.2009.

Expression and function of CXCL12/CXCR4 in rat urinary bladder with cyclophosphamide-induced cystitis

Lauren Arms,[2] Beatrice M. Girard,[2] and Margaret A. Vizzard,[1,2]

Departments of [1]Neurology and [2]Anatomy and Neurobiology, University of Vermont College of Medicine, Burlington, Vermont

Submitted 3 November 2009; accepted in final form 18 December 2009

Arms L, Girard BM, Vizzard MA. Expression and function of CXCL12/CXCR4 in rat urinary bladder with cyclophosphamide-induced cystitis. *Am J Physiol Renal Physiol* 298: F589–F600, 2010. First published December 23, 2009; doi:10.1152/ajprenal.00628.2009.—Chemokines, otherwise known as chemotactic cytokines, are proinflammatory mediators of the immune response and have been implicated in altered sensory processing, hyperalgesia, and central sensitization following tissue injury or inflammation. To address the role of CXCL12/CXCR4 signaling in normal micturition and inflammation-induced bladder hyperreflexia, bladder inflammation in adult female Wistar rats (175–250 g) was induced by injecting cyclophosphamide (CYP) intraperitoneally at acute (150 mg/kg; 4 h), intermediate (150 mg/kg; 48 h), and chronic (75 mg/kg; every 3rd day for 10 days) time points. CXCL12, and its receptor, CXCR4, were examined in the whole urinary bladder of control and CYP-treated rats using enzyme-linked immunosorbent assays (ELISAs), quantitative PCR (qRT-PCR), and immunostaining techniques. ELISAs, qRT-PCR, and immunostaining experiments revealed a significant ($P \leq 0.01$) increase in CXCL12 and CXCR4 expression in the whole urinary bladder, and particularly in the urothelium, with CYP treatment. The functional role of CXCL12/CXCR4 signaling in micturition was evaluated using conscious cystometry with continuous instillation of saline and CXCR4 receptor antagonist (AMD-3100; 5 μM) administration in control and CYP (48 h)-treated rats. Receptor blockade of CXCR4 using AMD-3100 increased bladder capacity in control (no CYP) rats and reduced CYP-induced bladder hyperexcitability as demonstrated by significant ($P \leq 0.01$) increases in intercontraction interval, bladder capacity, and void volume. These results suggest a role for CXCL12/CXCR4 signaling in both normal micturition and with bladder hyperreflexia following bladder inflammation.

urothelium; chemokines; cystometry; AMD-3100; bladder hyperreflexia

CHEMOKINES, chemotactic cytokines, are a large family of structurally and functionally related agents that are well-known mediators of immune responses and inflammatory processes (53, 57). More recently, however, studies suggest roles for chemokine signaling in sensory and nociceptive processes. Under physiological conditions, with the exception of CXCL12 (73), neuronal chemokine expression is sparse; however, following nerve injury or inflammation, expression of chemokines and associated receptors increases significantly in sensory neurons, glia, macrophages, infiltrating T cells, spinal cord, and dorsal root ganglia (DRG) (6, 7, 41, 53, 65, 67, 74). Additionally, elevated neuronal chemokine expression or exogenous application correlates with the maintenance of persistent pain while blockade of chemokine signaling attenuates pain behavior (6, 46, 49).

Address for reprint requests and other correspondence: M. A. Vizzard, Univ. of Vermont College of Medicine, Dept. of Neurology, D415A Given Research Bldg., Burlington, VT 05405 (e-mail: Margaret.Vizzard@uvm.edu).

Interstitial cystitis/painful bladder syndrome (IC/PBS) is a chronic bladder syndrome with symptoms of urgency, frequency, nocturia, and suprapubic and pelvic pain (51). IC/PBS patients have a lower threshold for sensing bladder volume and often experience pain at normal bladder pressures, which suggests altered sensory processing within the urinary tract and/or its innervation (20, 47). Although some theories exist as to the underlying mechanisms of this syndrome, the etiology remains largely unclear (18, 30, 32, 50, 51, 55). However, the majority of bladder biopsies from IC/PBS patients reveal some degree of inflammatory infiltration (56), suggesting that inflammatory mediators, including chemokines, may contribute to inflammatory-induced changes, including urinary bladder and sensory dysfunction.

Potential roles of chemokine/receptor signaling in the urinary bladder are emerging. Previous studies have shown that the expression of chemokines and/or receptors is increased following cyclophosphamide (CYP)-induced bladder inflammation (54, 66, 78). Recent studies demonstrated increased serum expression of chemokines in IC/PBS patients (54). Furthermore, in chemically induced colitis, CXCL12 is increased in the colon, and its main receptor, CXCR4, is increased in peripheral T cells and leukocytes (45). More recently, CXCR7 has been demonstrated as a second receptor binding to CXCL12 (79, 81). Blockade of CXCR4 reduces colonic inflammation (45) and attenuates somatic sensitivity (7). CYP causes bladder hyperreflexia and induces neurochemical (68, 69, 71, 83), organizational (69, 72), and electrophysiological (31, 77) changes within the bladder and bladder afferent neurons. Potential mediators of urinary bladder inflammation are numerous: cytokines (19, 40, 43), chemokines (54, 66, 78), neuropeptides (12, 68), neuroactive compounds (11), and growth factors (70, 76, 82).

The present study addresses CXCL12/CXCR4 expression and regulation in urinary bladder and micturition reflexes using a CYP-induced model of bladder inflammation. We determined *1*) expression and regulation of CXCL12 and its receptor CXCR4 in the urinary bladder using immunohistochemistry, quantitative PCR (qRT-PCR), and enzyme-linked immunosorbent assays (ELISA) with CYP-induced bladder inflammation of varying duration and *2*) the effects of CXCR4 blockade with AMD-3100, a compound known to specifically block CXCR4 (26, 44), on micturition reflexes using conscious cystometry with continuous intravesical instillation of saline in both CYP-treated and control (noninflamed) female rats. Parts of these studies have been published in abstract form (3).

MATERIALS AND METHODS

Animals

Adult female Wistar rats (150–250 g), purchased from Charles River Canada (St. Constant, PQ, Canada), were housed two per cage

and maintained in standard laboratory conditions with free access to food and water. The University of Vermont Institutional Animal Care and Use Committee approved all animal use procedures (protocol 08–085). Animal experimentation was carried out in accordance with the National Institutes of Health Guide for the Care and Use of Laboratory Animals.

Induction of CYP-Induced Cystitis

Rats were anesthetized with isoflurane (2%) and received intraperitoneal injection(s) of CYP (Sigma Aldrich, St. Louis, MO) to produce urinary bladder inflammation. To induce chronic bladder inflammation, CYP was injected (75 mg/kg ip) every 3rd day for 10 days with death occurring on the 10th day (16, 37, 38). To induce acute bladder inflammation, CYP was injected (150 mg/kg ip) with death occurring 4 or 48 h after injection (16, 37, 38). Control rats received no treatment. For conscious cystometry studies, rats received CYP as described with bladder function testing occurring 48 h after injection.

Preparation of Tissue Samples for ELISAs

Rats from all experimental groups (control, 4 h, 48 h, and chronic; $n = 4$) were killed with isoflurane (4%), a thoracotomy was performed, and the urinary bladder was harvested. Individual bladders were immediately weighed and solubilized in tissue protein extraction reagent (1 g tissue/20 ml; Pierce Biotechnology, Woburn, MA) and treated with complete protease inhibitor cocktail tablets (Roche, Indianapolis, IN) (14, 78). Tissue was homogenized using a Polytron homogenizer and centrifuged (10,000 rpm for 10 min). The resulting supernatant was used for CXCL12 protein quantification. Total protein was determined using the Coomassie Plus Protein Assay Reagent Kit (Pierce). CXCL12 was quantified using standard 96-well ELISA plates (R&D Systems, Minneapolis, MN) according to the manufacturer's recommendations.

ELISAs for CXCL12 in Urinary Bladder

Microtiter plates (R&D Systems) were coated with anti-CXCL12 antibody. Sample and standard solutions were run in duplicate. Horseradish peroxidase-streptavidin conjugate was used to detect the antibody complex. Tetramethylbenzidine was the substrate, and the enzyme activity was measured by the change in optical density. The standards generated produced a linear curve. The absorbance values of standards and samples were corrected by the subtraction of the background value (absorbance resulting from nonspecific binding). Samples were not diluted, and no samples fell below the detection limits of the assays.

Immunohistochemical Localization of CXCL12 and CXCR4 in the Urothelium

The bladders were rapidly dissected and placed in 4% paraformaldehyde followed by overnight incubation in 30% sucrose in 0.1 M PBS for cryoprotection. Tissue was frozen in optimal cutting temperature compound, sectioned (20 μm) on a freezing cryostat, and mounted directly on gelled (0.5%) microscope slides (14, 16). Sections were incubated overnight at room temperature in rabbit anti-CXCL12 (1:500; Santa Cruz Biotechnology, Santa Cruz, CA) or rabbit anti-CXCR4 (1:2,000; Sigma Aldrich). Antibodies were diluted in 1% goat serum and 0.1 M phosphate buffer. After overnight incubation, sections were washed (3 × 10 min) with 0.1 M PBS (pH 7.4). Sections were then incubated with Cy3-conjugated, species-specific secondary antibodies for 2 h at room temperature followed by washes (3 × 10 min) with PBS and coverslipping with Citifluor (Citifluor). Control tissue sections were incubated with 1% goat serum and 0.1 M phosphate buffer alone (no primary antibody), followed by normal washing and incubation with secondary antibodies to evaluate background staining levels. In the absence of primary antibody, no positive immunostaining was observed.

Visualization and Semiquantitative Analysis of CXCL12 and CXCR4 in Urothelium

CXCL12- and CXCR4-immunoreactivity (IR) staining in bladder sections was visualized, and images were captured using an Olympus fluorescence photomicroscope. The filter was set with an excitation range of 560–569 nm and emission range of 610–655 nm for visualization of Cy3. Images were captured, acquired in tiff format, and imported into Meta Morph image analysis software (version 4.5r4; University Imaging, Downingtown, PA) (14, 16). The free hand drawing tool was used to select the urothelium, and the urothelium was measured in total pixel areas (14, 16). A threshold encompassing an intensity range of 100–250 grayscale values was applied to the region of interest in the least brightly stained condition first. The threshold was adjusted for each experimental series using concomitantly processed negative controls as a guide for setting background fluorescence. The same threshold was subsequently used for all images. Immunoreactivity was considered to be positive only when the staining for the marker of interest (CXCL12 or CXCR4) exceeded the established threshold. Percent marker expression above threshold in the total area selected was calculated.

Assessment of Immunohistochemical Staining in Urinary Bladder Regions

Immunohistochemistry and subsequent evaluation of CXCL12- and CXCR4-IR in bladder sections or whole mount preparations were performed on control and experimental tissues simultaneously to reduce the incidence of staining variation that can occur between tissues processed on different days. Staining in experimental tissue was compared with that in experiment-matched negative controls. Urinary bladder sections or whole mounts exhibiting immunoreactivity that was greater than background level in experiment-matched negative controls were considered positively stained. Control sections incubated in the absence of primary or secondary antibody were also processed and evaluated for specificity or background staining levels. In the absence of primary antibody, no positive immunostaining was observed. Preabsorption of CXCL12 or CXCR4 antisera with appropriate immunogen (CXCL12: 1 μg/ml; CXCR4: 1–3 μg/ml) reduced staining to background levels.

During pilot studies, additional antibodies for both CXCL12 (1:100; R&D Systems) and CXCR4 (1:1,000; MBL, Woburn, MA) were evaluated to determine if staining was comparable in urinary bladder with CYP-induced cystitis. The pattern of staining observed for both CXCL12 and both CXCR4 antibodies in urinary bladder after CYP treatment was consistent.

Immunohistochemical Localization of CXCL12 and CXCR4 in Suburothelial Nerve Plexus in Urinary Bladder Whole Mounts

The urinary bladder was dissected rapidly and placed in oxygenated (95% O_2 and 5% CO_2) physiological saline solution (in mmol: 119.0 NaCl, 4.7 KCl, 24.0 $NaHCO_3$, 1.2 KH_2PO_4, 1.2 $MgSO_4 \cdot 7H_2O$, and 11.0 glucose) (14, 37, 78). Starting at the urethra, a midline incision was made through the bladder, and it was pinned flat onto a Sylgard-coated dish, maximally stretched, and then fixed in 2% paraformaldehyde + 0.2% picric acid for 1.5 h. After fixation, the urothelium was separated from the detrusor layer using fine-tip forceps, iris scissors, and a dissecting microscope as previously described (14, 37, 78). Notches were made in the region of the bladder neck to track orientation and assess regional immunoreactivity of the bladder. Urothelium and bladder musculature were processed for CXCL12- and CXCR4-IR as described previously. In some whole mounts processed for CXCL12- and CXCR4-IR, nerve fibers in the suburothelial nerve plexus were also stained with the pan-neuronal marker protein gene product (PGP9.5, 1: 3,000; AbD Serotec, Raleigh, NC) and stained with Cy2-conjugated species-specific secondary antibodies.

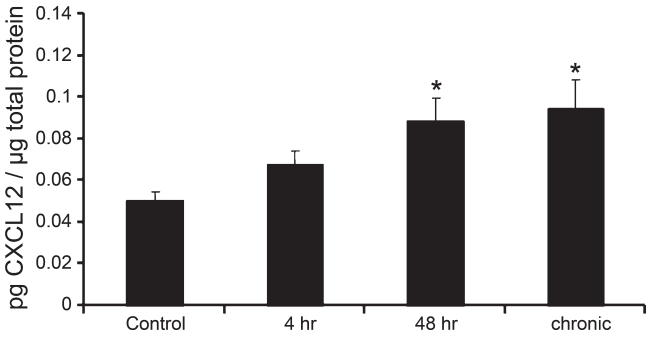

Fig. 1. Time-dependent changes in CXCL12 protein expression in whole urinary bladder following cyclophosphamide (CYP) treatment as determined with enzyme-linked immunosorbent assays (ELISAs). CXCL12 expression increased significantly (*$P \leq 0.01$) at 48 h and chronic time points compared with control urinary bladders; $n = 4$ for control and each experimental condition.

Visualization of CXCL12- and CXCR4-IR in Suburothelial Plexus in Bladder Whole Mounts

Whole mount tissue from control and experimental groups were examined with a multiband filter set for simultaneous visualization of the Cy3 and Cy2 fluorophores. Cy2 was viewed using a filter with an excitation range of 447–501 nm and an emission range from 510 to 540 nm. Double-labeling in whole mount preparations of urothelium and detrusor was assessed by confocal laser scanning microscopy (Bio-Rad Laboratories and Zeiss LSM 510 Meta, Carl Zeiss; see Ref. 38). For each z-axis interval (1–2 μm), tissue sections were scanned two times using argon lasers with specific excitation wavelengths, and sequential images were captured for computer-generated overlay and analysis.

CXCL12 and CXCR4 Transcript Expression in Urinary Bladder Using Real-Time qRT-PCR

Bladders were harvested, and the urothelium was separated from the detrusor as described above. Total RNA was extracted using the STAT-60 total RNA/mRNA isolation reagent (Tel-Test "B", Friendswood, TX) as previously described (22, 38). One to 2 mg of RNA per sample were used to synthesize cDNA using SuperScript II reverse transcriptase and random hexamer primers with the SuperScript II

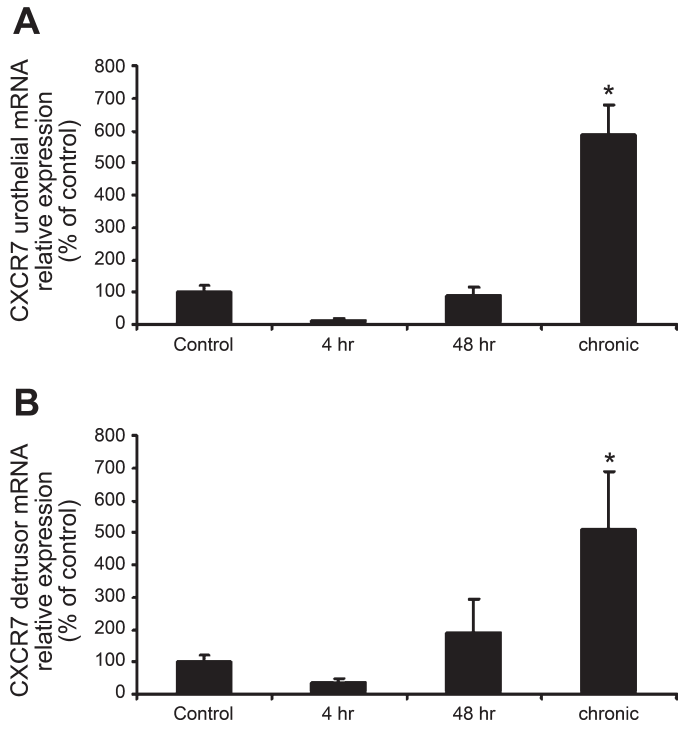

Fig. 3. Time-dependent and regional changes in CXCR7 mRNA expression in urinary bladder as detected by qRT-PCR. CXCR7 mRNA expression increased significantly in both the urothelium (*A*; *$P \leq 0.05$) and the detrusor (*B*; *$P \leq 0.05$) following chronic CYP treatment but not 4 or 48 h CYP treatment (n = 5–7 for each group).

Preamplification System (Invitrogen, Carlsbad, CA) in a 20-μl final reaction volume. Amplification of cDNA was performed using oligonucleotide primers specific for CXCL12, CXCR4, CXCR7, or L32. Oligonucleotide primer sequences were as follows: TGCATCAGTGACGGTAAGCCA (upper, CXCL12 130U21), ATCCACTTTAATTTCGGGTCAA (lower, CXCL12 296L22), TCCTGCCCACCATCTATTTTATC (upper, CXCR4 185U23), ATGATATGCACAGCCTTACAT (lower, CXCR4 390L21), ACGTGCAAGATCACACACCTCAT

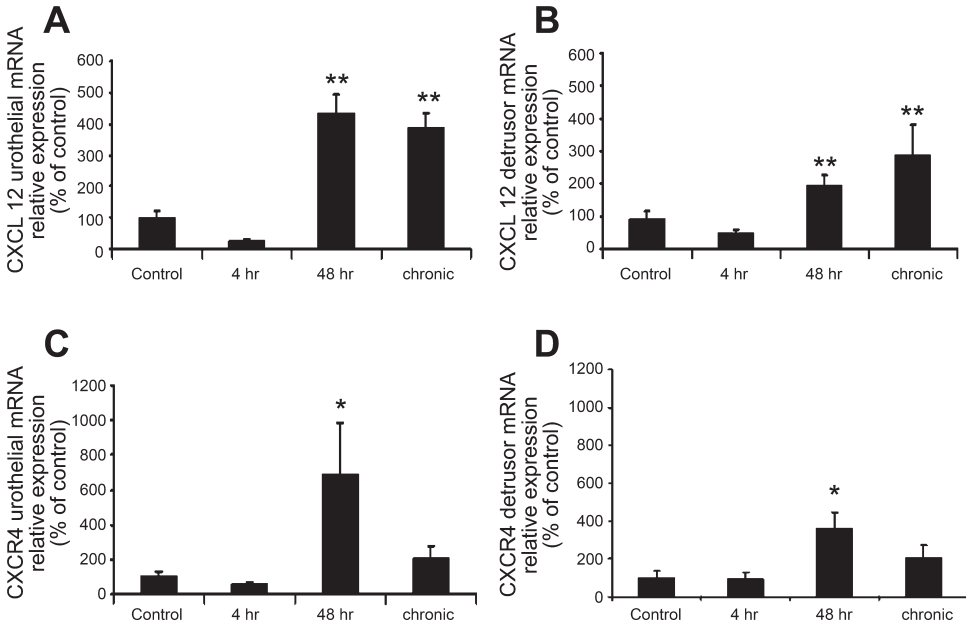

Fig. 2. Time-dependent and regional changes in CXCL12 and CXCR4 mRNA expression in urinary bladder as detected by quantitative PCR (qRT-PCR). Following 48 h and chronic CYP treatment, CXCL12 mRNA expression was significantly increased in both the urothelium (*A*; **$P \leq 0.01$) and the detrusor (*B*; **$P \leq 0.01$). CXCR4 mRNA expression was increased significantly after 48 h CYP treatment in both the urothelium (*C*; *, $P \leq 0.05$) and the detrusor (*D*; *$P \leq 0.05$); n = 5–7 for each group.

(upper, rCXCR7 346U23), and GATCTTCCGGCTGCTGTGTT-TCT (lower, rCXCR7 737L23).

The qRT-PCR standards for all transcripts were prepared with the amplified CXCL12, CXCR4, CXCR7, and L32 cDNA products ligated directly into pCR2.1 TOPO vector using the TOPO TA cloning kit (Invitrogen). The nucleotide sequences of the inserts were verified by automated fluorescent dideoxy dye terminator sequencing (Vermont Cancer Center DNA Analysis Facility). To estimate the relative expression of the receptor transcripts, 10-fold serial dilutions of stock plasmids were prepared as quantitative standards. The range of standard concentrations was determined empirically.

Real-time qRT-PCR was performed using SYBR Green I detection (22, 38). cDNA templates, diluted 10-fold to minimize the inhibitory effects of the reverse transcription reaction components, were assayed using HotStart-IT SYBR Green qPCR Master Mix (USB, Cleveland, OH) containing 5 mM $MgCl_2$, 0.4 mM dATP, dGTP, dCTP, and dTTP, HotStart-IT Taq DNA polymerase, and 300 nM of each primer in a final 25-ml reaction volume. The real-time qRT-PCR was performed on an Applied Biosystems 7500 Fast real-time PCR system (Applied Biosystems, Foster City, CA) (22, 38) using the following standard conditions: *1*) 94°C for 2 min; *2*) amplification over 40 cycles at 94°C for 15 s and 58–60°C depending on primer set for 30 s.

The amplified product from these amplification parameters was subjected to SYBR Green I melting analysis by ramping the temperature of the reaction samples from 60 to 95°C. A single DNA melting profile was observed under these dissociation assay conditions, demonstrating amplification of a single unique product free of primer dimers or other anomalous products.

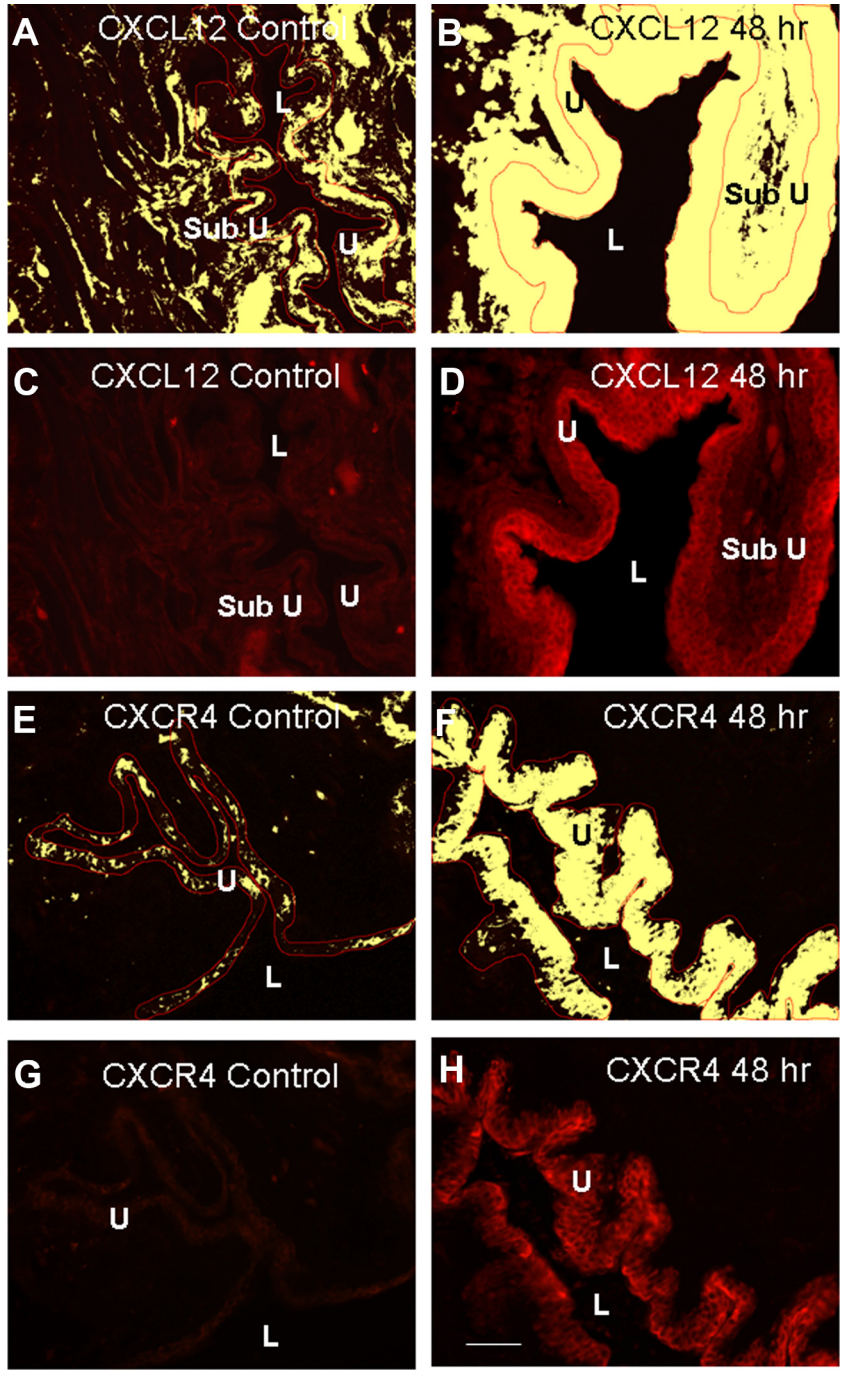

Fig. 4. Regulation of CXCL12 (*A–D*) and CXCR4 (*E–H*) expression in cryostat sections of urinary bladder after CYP treatment. The urothelium was outlined in red, and images were thresholded (*A*, *B*, *E*, and *F*). All pixels above threshold are depicted in yellow. Corresponding fluorescence images of CXCL12 expression in control or after 48 h CYP treatment are shown in *C* and *D*, respectively. Fluorescence images of CXCR4 expression in urinary bladder of control or after 48 h CYP treatment are shown in *G* and *H*, respectively. L, lumen; U, urothelium; Sub U, suburothelium. Calibration bar represents 50 μm.

For data analyses, a standard curve was constructed by amplification of serially diluted plasmids containing the target sequence. Data were analyzed at the termination of each assay using the Sequence Detection Software version 1.3.1 (Applied Biosystems, Norwalk, CT). In standard assays, default baseline settings were selected. The increase in SYBR Green I fluorescence intensity (ΔRn) was plotted as a function of cycle number, and the threshold cycle was determined by the software as the amplification cycle at which the ΔRn first intersects the established baseline. All data are expressed as the relative quantity of the gene of interest normalized to the relative quantity of housekeeping gene. Control samples were set equal to 100%.

Intravesical Catheter Implant

A lower midline abdominal incision was performed under general anesthesia with 2–3% isoflurane using aseptic techniques (13, 29, 39). The end of polyethylene tubing (PE-50; Clay Adams, Parsippany, NJ) was flared with heat and inserted in the dome of the bladder and secured in place with a 6–0 nylon purse-string suture (13, 29, 39). The distal end of the tubing was sealed and tunneled subcutaneously to the back of the neck where it was externalized, out of the animal's reach (13, 29, 39). Rats received buprenorphine (0.05 mg/kg sc) starting at the time of surgery and then every 8–12 h postoperatively for a total of four doses. Animals were maintained for 72 h after surgery before conscious cystometry was initiated to ensure complete recovery.

Conscious Cystometry with Continuous Intravesical Infusion of Saline and CXCR4 Blockade

The effects of CXCR4 blockade on bladder function in control (no inflammation) and CYP-treated rats (48 h) were evaluated by pharmacological receptor blockade with infusion of AMD-3100 (5 μM; Sigma Aldrich), known to specifically block CXCR4 (26, 44) using conscious cystometry and continuous infusion of intravesical saline. During cystometry, unrestrained and conscious rats were placed in a recording cage over a scale and pan to collect and measure voided urine. To elicit repetitive bladder contractions, room temperature saline was infused at a constant rate (10 ml/h). At least six reproducible micturition cycles were recorded after an initial stabilization period (25–30 min). Intravesical pressure changes were recorded using a Small Animal Cystometry System (Med Associates, St. Albans, VT) (13, 38). Baseline resting pressure, pressure threshold for voiding, maximal voiding pressure, and intercontraction interval were measured before AMD-3100 instillation. Nonvoiding bladder contractions (NVCs), defined as rhythmic intravesical pressure increases 7 cmH_20 above baseline without the release of fluid from the urethra, were also determined per voiding cycle. Bladder capacity was measured as the amount of saline infused in the bladder at the time when micturition commenced (10, 27).

To evaluate the effects of CXCR4 blockade on bladder function, immediately following the baseline recordings, rats were anesthetized (1–2% isoflurane), and AMD-3100 (5 μM), known to specifically block CXCR4 (25, 41), was intravesically infused for 30 min. The concentration selected for evaluation was based on published studies (35). Before intravesical drug infusion, the bladder was manually emptied via the Credé maneuver. Bladders were then infused with ~1 ml (less than bladder capacity to not elicit a bladder contraction and expulsion of instillate) of AMD-3100 (5 μM) according to prior published studies (13, 39). Rats remained anesthetized (1–2% isoflurane) to subdue the micturition reflex and prevent expulsion of the CXCR4 receptor antagonist from the bladder. Immediately following drug treatment, bladder function testing was repeated. To avoid potential variation resulting from circadian rhythms, experiments were conducted at similar times of the day (17). At the conclusion of the study, rats were killed as described above. To determine if the experimental design of the studies (i.e., baseline bladder function recordings, anesthesia and intravesical drug instillation, additional bladder function recordings) could affect cystometric recordings, additional rats (control, no inflammation, and 48 h CYP-treated) underwent baseline recordings, anesthesia and intravesical saline instillation, and additional cystometric analyses. These studies with identical experimental design and intravesical saline instillation revealed no changes in cystometric parameters analyzed (data not shown).

Exclusion Criteria

Rats were removed from the study when adverse events occurred that included 20% reduction in body weight postsurgery, a significant postoperative event, lethargy, pain, or distress not relieved by our Institutional Animal Care and Use Committee-approved regimen of postoperative analgesics or hematuria in control rodents (13, 39). In the present study, no rats were excluded from the study or from analysis because of any of these exclusion criteria. In addition, behavioral movements such as grooming, standing, walking, and defecation rendered bladder pressure recordings during these events unusable.

Materials

AMD-3100 was purchased from Sigma Aldrich, prepared as concentrated stock solutions, aliquoted, and stored at −20°C until usage. Aliquots were diluted with saline to achieve final concentration.

Figure Preparation

Digital images were obtained using a charge-coupled device camera (MagnaFire, Optronics; Optical Analysis) and LG-3 frame grabber attached to an Olympus microscope (Optical Analysis, Nashua, NH). Exposure times were held constant when acquiring images from

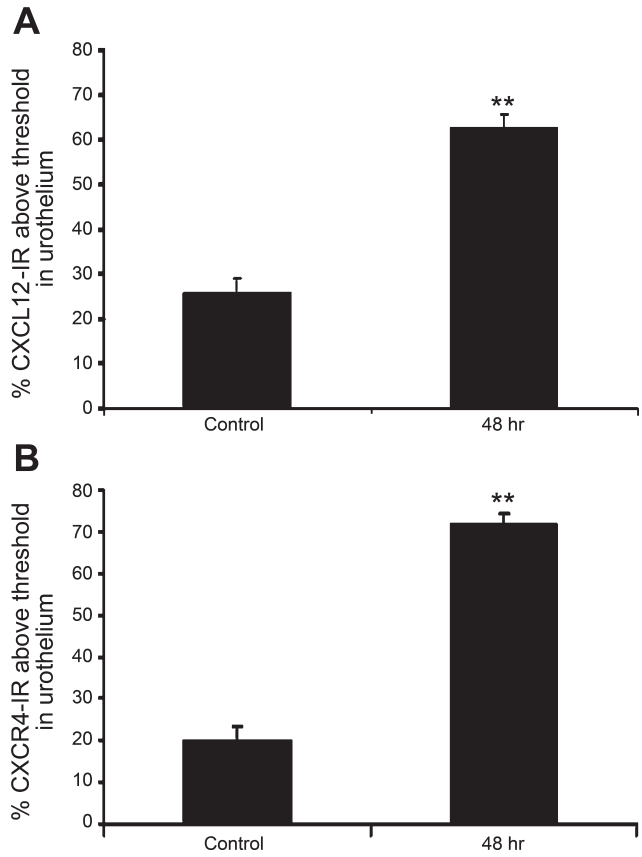

Fig. 5. Summary histogram of CXCL12 (*A*)- and CXCR4-immunoreactivity (IR) (*B*) expression in the urothelium of the urinary bladder of control rats and those treated with CYP (48 h). Values are means ± SE (n = 3–8). **$P \leq 0.01$.

control and experimental animals processed and analyzed on the same day. Images were imported into Adobe Photoshop 8.0 (Adobe Systems, San Jose, CA) where groups of images were assembled and labeled.

Statistical Analyses

All values represent means ± SE. Data were compared with ANOVA or repeated measures ANOVA, where appropriate. When F ratios exceeded the critical value ($P \leq 0.05$), the Newman-Keul's or Dunnett's post hoc tests were used to compare group means.

RESULTS

CXCL12 Protein Expression in the Rat Urinary Bladder with CYP-Induced Cystitis

CXCL12 protein expression in the whole urinary bladder increased significantly ($P \leq 0.01$) after 48 h (1.8-fold) and chronic (1.9-fold; Fig. 1) CYP treatment as determined with ELISAs. CXCL12 bladder expression with 48 h CYP treatment did not differ from chronic CYP treatment. No change in CXCL12 urinary bladder expression was observed with 4 h CYP treatment.

CXCL12, CXCR4, and CXCR7 mRNA Expression in the Urinary Bladder of Rats with and without CYP-Induced Cystitis

qRT-PCR demonstrated a significant ($P \leq 0.01$) increase in CXCL12 mRNA in both the urothelium and detrusor with 48 h and chronic CYP treatment but not 4 h CYP treatment (Fig. 2, *A* and *B*). CXCR4 mRNA was increased significantly ($P \leq 0.05$) with 48 h CYP treatment in both the urothelium and detrusor (Fig. 2, *C* and *D*). No change in CXCR4 mRNA expression was observed at 4 h or chronic CYP treatment time points (Fig. 2, *C* and *D*). CXCR7 mRNA increased significantly ($P \leq 0.05$) after chronic CYP treatment in both the urothelium and the detrusor (Fig. 3, *A* and *B*). No change in CXCR7 mRNA expression was observed at the 4- or 48-h CYP treatment time points (Fig. 3, *A* and *B*).

CXCL12- and CXCR4-IR in Urinary Bladder with CYP-Induced Cystitis

Urinary bladder sections. Basal CXCL12-IR expression was present in the urothelium in all urothelial layers (basal, intermediate, and apical) and lamina propria and more diffusely in the detrusor in control (no inflammation) urinary bladder (Fig. 4, *A* and *C*). When examining CXCL12-IR following CYP treatment, we focused on the 48-h time point because it is the earliest CYP treatment where we observed an increase in CXCL12 mRNA and protein expression in the whole urinary bladder. Additionally, neither CXCL12 mRNA nor the protein expression levels differed from the chronic CYP treatment time point. Following 48 h CYP treatment, CXCL12-IR expression was robust in the urothelium and lamina propria (Fig. 4, *B* and *D*). We focused our analyses of CXCL12 expression in the urothelium because expression was most dramatically upregulated in the urothelium with CYP treatment. Urothelial CXCL12-IR was significantly ($P \leq 0.01$) increased (2.4-fold) with 48 h CYP-treatment (Fig. 5*A*). In control (no inflammation) bladders, CXCR4-IR expression was virtually absent in the lamina propria and detrusor, but basal urothelial CXCR4-IR expression was present (Fig. 4, *E* and *G*). Following 48 h CYP treatment, urothelial CXCR4-IR increased significantly ($P \leq 0.01$; 3.5-fold; Fig. 4, *F* and *H* and Fig. 5*B*).

Bladder whole mounts. CXCL12- or CXCR4-IR in the suburothelial nerve plexus was not observed in control or CYP-treated whole mount bladder preparations. Multiple attempts ($n = 6$–10) with different species-specific secondary antibodies to visualize CXCL12- or CXCR4-IR in the suburothelial plexus were not successful (data not shown). Furthermore, despite PGP immunostaining of the suburothelial nerve plexus, colocalization with either CXCL12- or CXCR4-IR was not observed with confocal or indirect immunofluorescence

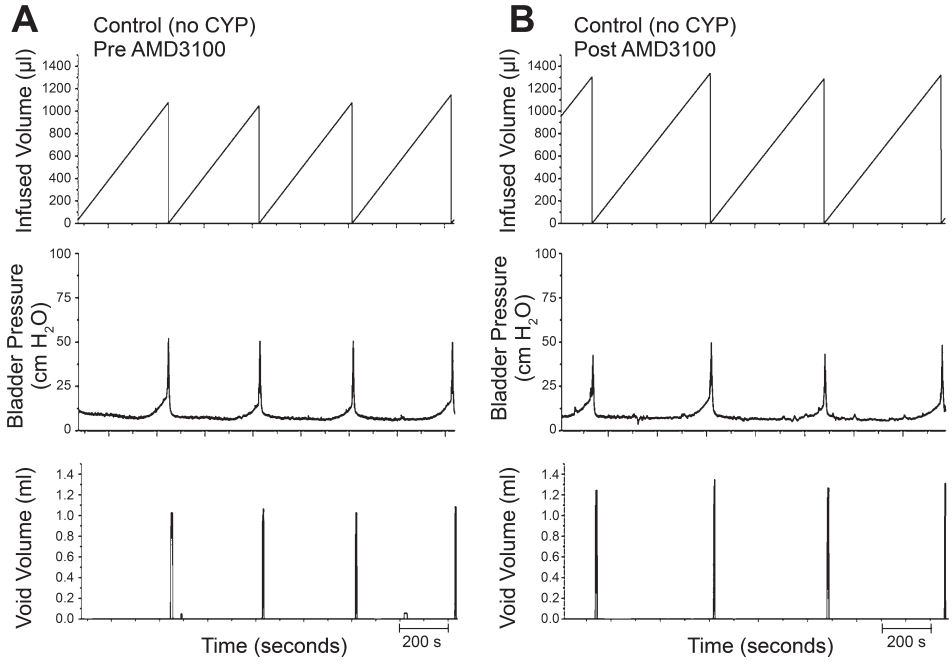

Fig. 6. Representative cystometrogram recordings of effects of CXCR4 receptor blockade in control (no inflammation) rats using continuous intravesical infusion of saline. Pre-AMD-3100 (*A*) and post-AMD-3100 (*B*) drug treatments in control rats (no CYP treatment) with continuous intravesical instillation of saline. CXCR4 receptor blockade with intravesical infusion of AMD-3100 (5 μM) increased both bladder capacity (measured as the amount of saline infused in the bladder at the time when micturition commenced) and void volume compared with pretreatment conditions (*A*). Bladder function recordings in *A* and *B* are recorded from the same rat.

techniques (data not shown). In contrast, whole mount preparations exhibited urothelial, lamina propria, and detrusor smooth muscle staining for CXCL12 or CXCR4 consistent with staining observed in cryostat bladder sections (data not shown).

CXCR4 Blockade with Intravesical Infusion of AMD-3100 using Conscious Cystometry in Rats with and without CYP-Induced Cystitis

Control (no inflammation). Conscious cystometry was performed in control rats before drug treatment to establish baseline voiding frequency, bladder capacity, and void volume (Figs. 6*A* and 7). Following intravesical infusion of AMD-3100 (5 μM), a CXCR4 receptor antagonist, the same rats exhibited decreased voiding frequency coupled with an increase (1.3-fold) in both bladder capacity, as measured as the amount of saline infused in the bladder at the time when micturition commenced ($P \leq 0.01$; Figs. 6*B* and 7), and duration of intercontraction interval ($P \leq 0.01$; Figs. 6*B* and 7), and an increase (1.3-fold) in void volume ($P \leq 0.05$; Figs. 6*B* and 7). There were no changes in threshold, filling, or peak micturition pressures following AMD-3100 treatment in control rats (Table 1).

CYP treatment. As previously demonstrated (13, 28, 29, 39), CYP treatment (48 h) increased void frequency and decreased bladder capacity, intercontraction interval, and void volume (Figs. 8*A* and 9). Additionally, CYP treatment increased ($P \leq 0.01$) filling, threshold, and micturition pressures (Table 1). Following intravesical infusion of AMD-3100 (5 μM), the same rats exhibited decreased voiding frequency and significantly ($P \leq 0.001$) increased bladder capacity (1.9-fold), as measured as the amount of saline infused in the bladder at the time when micturition commenced, intercontraction interval (1.9-fold), and increased void volume (2.2-fold; Figs. 8*B* and 9). There were no changes in threshold, filling, or peak micturition pressures following AMD-3100 treatment in CYP-treated (48 h) rats (Table 1).

Table 1. *Threshold and peak micturition and filling pressures during conscious cystometry for control and 48 h CYP-treated rats both pre- and post-AMD-3100 treatment*

	Threshold Pressure	Peak Micturition Pressure	Filling Pressure
Control			
Pre-AMD	14.2 + 0.7	51.7 + 1.6	10.6 + 0.6
Post-AMD	14.0 + 0.9	47.7 + 2.0	9.7 + 0.6
48 h CYP			
Pre-AMD	24.3 + 1.1*	65.4 + 3.2*	23.1 + 1.1*
Post-AMD	23.6 + 1.2	74.4 + 5.1	22.5 + 1.2

Values presented are means ± SE; $n = 4–6$ rats in each group. Units are cmH_2O. CYP, cyclophosphomide; AMD, AMD-3100. No pressure changes were observed within experimental groups (i.e., control pre-AMD vs. post-AMD or CYP pre-AMD vs. post-AMD) following AMD-3100 (5 μM) instillation; however, CYP treatment (48 h) significantly (*$P \leq 0.05$) increased threshold and peak micturition and filling pressures when compared with control rats.

NVCs (increases in baseline pressure with an amplitude $\geq 7 cmH_2O$ without the expulsion of urine) occurred very infrequently in the evaluated rats with CYP treatment before or after intravesical infusion of AMD-3100. Therefore, the effect of AMD-3100 on NVCs was not assessed.

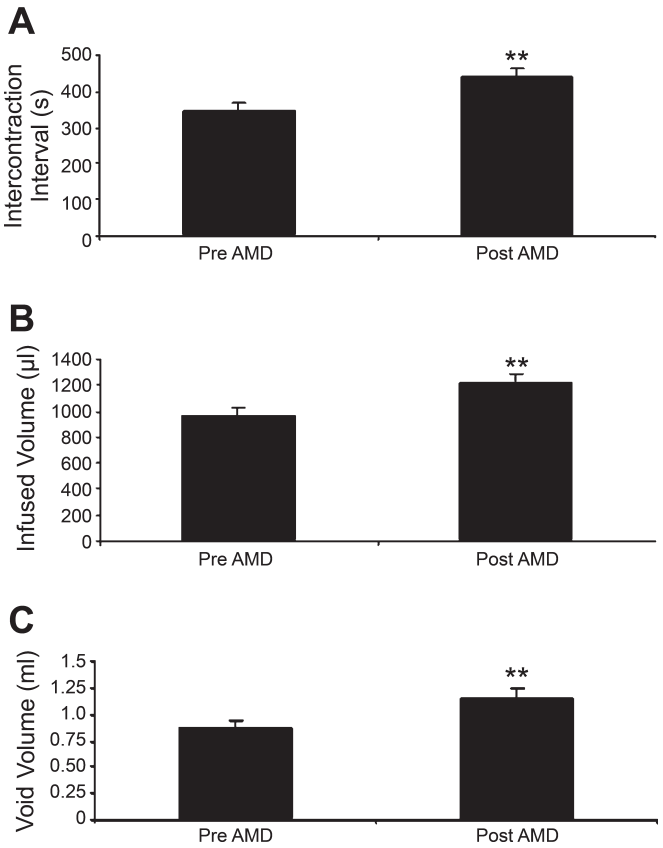

Fig. 7. Summary histograms of the effects of CXCR4 receptor blockade with AMD-3100 intravesical infusion in control rats (no CYP treatment). *A*: infusion of AMD-3100 (5 μM) significantly (**$P \leq 0.01$) increased intercontraction interval. *B*: bladder capacity was also significantly (**$P \leq 0.01$) increased along with a significantly (*$P \leq 0.05$) increased void volume (*C*). Values are means ± SE ($n = 4–6$).

DISCUSSION

These studies demonstrate several novel findings with respect to chemokine/receptor regulation and function in micturition reflexes under normal or inflamed bladder conditions in female rats. We have previously shown CYP-induced changes in urinary bladder expression of the chemokine/receptor pair: CX3CL1/CX3CR1 (78). In the present studies, we demonstrate that a second chemokine receptor pair, CXCL12/CXCR4 *1*) has low basal expression in the urinary bladder; *2*) increases in the urinary bladder following CYP treatment of varying duration; *3*) exhibits strong expression in the urothelium following CYP-induced cystitis; and *4*) plays a role in bladder function in both normal (no CYP) and CYP-treated rats. CXCR4 blockade at the level of the urinary bladder increased bladder capacity and void volume in normal and, to a greater extent, in CYP-treated rats. To the best of our knowledge, these studies are the first to demonstrate roles for chemokine/receptor signaling in bladder function. Therefore, chemokines may represent a novel class of potential molecular targets for pharmaceutical intervention with respect to bladder inflammation.

IC/PBS is a chronic bladder syndrome with symptoms of urgency, frequency, nocturia, and suprapubic and pelvic pain (51). Although the etiology and pathogenesis of IC are unknown, numerous theories, including infection, autoimmune disorder, toxic urinary components, deficiency in bladder wall

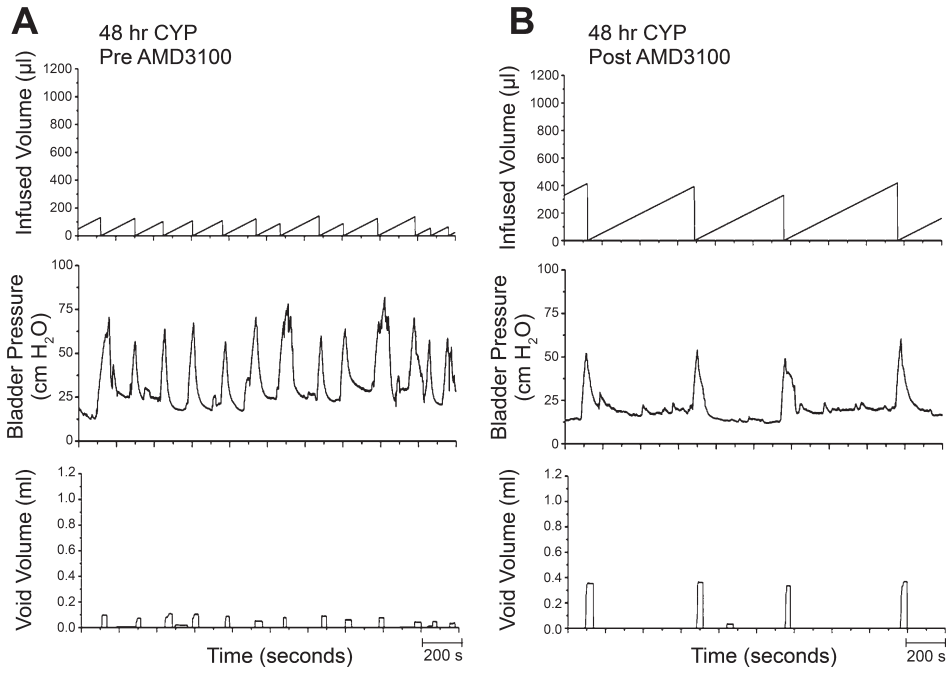

Fig. 8. Representative cystometrogram recordings of effects of CXCR4 receptor blockade in CYP-treated (48 h) rats using continuous intravesical infusion of saline. Pre-AMD-3100 (*A*) and post-AMD-3100 (*B*) drug treatments in 48 h CYP-treated rats with continuous intravesical instillation of saline. CXCR4 receptor blockade with intravesical infusion of AMD-3100 (5 μM) increased both bladder capacity (measured as the amount of saline infused in the bladder at the time when micturition commenced) and void volume compared with pretreatment conditions (*A*). Bladder function recordings in *A* and *B* are recorded from the same rat.

lining, and neurogenic causes, have been proposed (18, 30, 32, 50, 51, 55). We have hypothesized that pain associated with IC/PBS involves alteration of visceral sensation/bladder sensory physiology. Altered visceral sensations from the bladder (i.e., pain at low or moderate bladder filling) that accompany IC/PBS may be mediated by many factors, including changes in the properties of peripheral bladder afferent pathways such that bladder afferent neurons respond in an exaggerated manner to normally innocuous stimuli (allodynia). These changes may be mediated, in part, by inflammatory changes in the urinary bladder. Potential mediators of urinary bladder inflammation are numerous: cytokines (19, 40, 43), neuropeptides (12, 68), neuroactive compounds (11), growth factors (70, 76, 82), and chemokines (54, 66, 78). Increased serum levels of chemokines (e.g., CXCL9-CXCL11) in IC/PBS patients have been demonstrated (54).

Using the CYP-induced bladder inflammation model (16, 37), we aimed to characterize further the role of immune mediators, specifically chemokines, in the development and/or maintenance of altered bladder sensory physiology associated with urinary bladder inflammation. Chemokines are mediators of the innate immune response and assert protective effects by attracting leukocytes to sites of injury and by initiating extravasation and developing guiding chemotactic gradients (53, 57). Recently, mediators of the immune response, including chemokines, have received considerable attention for their potential role in heightened sensory processing and pain (53, 73). For example, exogenous administration of chemokines induces thermal hyperalgesia and mechanical allodynia (46, 49, 65). Additionally, in a model of neuropathic pain, hyperalgesia occurs concomitantly with increased chemokine signaling, through CXCR4 specifically (6). In contrast, antagonists to chemokine receptors can reduce nociceptive behavior (6, 46), and certain chemokine knockout mice fail to develop somatic sensitivity (1). Recently, Foster et al. (21) showed that hindpaw mechanical hypersensitivity induced by unilateral injections of acidic saline in the pelvic floor muscles of rats can be ameliorated by administration of AMD-3100. CYP-induced bladder inflammation in mice and rats is associated with increased, referred somatic sensitivity (13, 24, 59). Effects of CXCR4 receptor blockade on CYP-induced referred somatic sensitivity were not evaluated in this study due to experimental procedures including a laparotomy. Studies to assess the contribution of CXCR4 to CYP-induced referred somatic sensitivity would, however, be of interest in the future. Thus chemokine signaling may contribute to altered somatic sensation, but roles in bladder sensory physiology have not yet been considered.

Previous studies demonstrated increased bladder chemokine expression following CYP treatment (66, 78). Fractalkine (CX3CL1) and fractalkine receptor (CX3CR1) expression were increased in the urothelium with CYP-induced cystitis (48 h and chronic). Similar to the present studies with CXCL12/CXCR4, fractalkine and fractalkine receptor were upregulated in the urothelium, with little effect being observed in the detrusor smooth muscle (78). Furthermore, neither CX3CL1/CX3CR1 nor CXCL12/CXCR4 was expressed in the suburothelial nerve plexus (78). Previous studies by Vera et al. (66) demonstrated increased CXCR4 expression and altered distribution in the urothelium of male Sprague-Dawley rats treated chronically with CYP. However, no increased expression of CXCL12 was noted in the bladder with CYP treatment (66). Furthermore, basal expression of CXCR4 in urothelium of control (no CYP) was greater (66) than that observed in the present study. Differences in CXCR4 and CXCL12 bladder expression between the study by Vera et al. (66) and the current study may be because of gender and strain differences in the rats studied and/or CYP dosing differences. Gender differences may be very likely given observations that estrogen regulates chemokine/receptor expression (58). The present studies extend previous studies (54, 66, 78) by demonstrating regulation and function of CXCL12/CXCR4 signaling in the urinary bladder with urinary bladder inflammation induced by

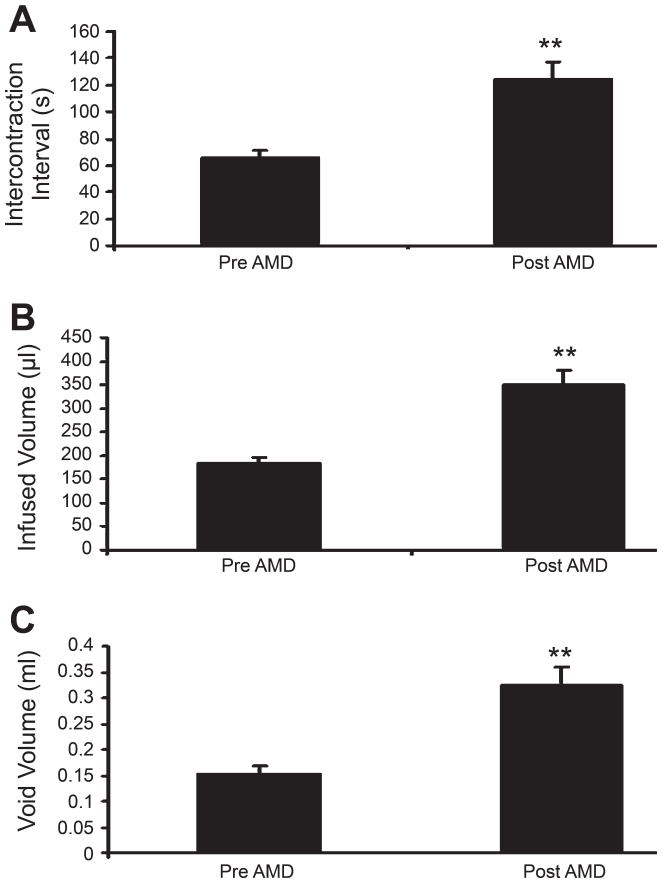

Fig. 9. Summary histograms of effects of CXCR4 receptor blockade with AMD-3100 intravesical infusion in 48 h CYP-treated rats. *A*: infusion of AMD-3100 (5 μM) significantly (**$P \leq 0.01$) increased intercontraction interval. *B*: bladder capacity was also significantly (**$P \leq 0.01$) increased along with a significantly (**$P \leq 0.01$) increased void volume (*C*). Values are means ± SE ($n = 6$).

CYP treatment. Increases in CXCL12 and its cognate receptor CXCR4 were observed in the urinary bladder following CYP treatment using multiple techniques, including qRT-PCR, ELISAs, and immunostaining.

Blockade of CXCR4 with a CXCR4 receptor antagonist, AMD-3100, reduced CYP-induced bladder hyperreflexia as evidenced by increased bladder capacity and decreased voiding frequency. In these studies, AMD-3100 is most likely acting at the level of the urothelium for several reasons: *1*) both mRNA and histological analyses showed that the greatest expressional increase for both CXCL12 and CXCR4 following CYP treatment was in the urothelium; *2*) histologically, CXCR4 had a restricted presentation, being expressed only in the urothelium in both control and CYP-treated bladders; and *3*) repeated attempts did not demonstrate CXCL12- or CXCR4-IR in the suburothelial nerve plexus. Furthermore, CXCR4 receptor blockade with AMD-3100 also significantly increased bladder capacity in control animals (no inflammation) that, without CYP treatment, should have an intact urothelium. The urothelium creates an impermeable barrier and has the highest junction potential of any cell type (75). Thus drug penetration through the urothelium to underlying structures (e.g., suburothelial plexus or detrusor smooth muscle) without use of a disrupting agent (e.g., protamine sulfate) is unlikely (15, 39). Changes in bladder function following AMD-3100 treatment in control animals should not be surprising, since bladders from these animals exhibit basal urothelial CXCL12 and CXCR4 expression. The magnitude of the increase in bladder capacity observed in control animals following AMD-3100 infusion was less than that observed in CYP-treated rats following AMD-3100 infusion. The increased magnitude of the change elicited with CXCR4 receptor blockade in CYP-treated rats may be because of: *1*) increased CXCL12 and CXCR4 expression in the urinary bladder following CYP treatment and *2*) a more prominent role for CXCL12/CXCR4 signaling in bladder function during inflammation.

AMD-3100 is a selective CXCR4 antagonist (26, 44); however, potential actions of CXCL12 through a second receptor, CXCR7, must also be considered (23). Balabanian et al. (5) showed that CXCL12 also binds CXCR7 in T lymphocytes and that this interaction partially mediates chemotaxis. In this study, we demonstrate using qRT-PCR studies that CXCR4 and CXCR7 mRNA expression is regulated in the urinary bladder following CYP-induced cystitis. However, the regulation of CXCR7 mRNA expression in urinary bladder with CYP treatment differs from that observed for CXCR4. CXCR4 mRNA expression is significantly increased in urinary bladder with 48 h CYP treatment. In contrast, CXCR7 transcripts significantly increase in urinary bladder with chronic CYP treatment but not with 4 or 48 h CYP treatment. Effects of AMD-3100 were observed when evaluated in 48 h CYP treated rats, consistent with blockade of CXCR4. Although CXCR7 mRNA expression did not increase with 48 h CYP treatment, basal urinary bladder expression of CXCR7 may be sufficient to contribute to the observed changes in bladder function. Although AMD-3100 is a selective CXCR4 antagonist (26, 44), AMD-3100 can act as a substantially weaker CXCR7 antagonist (42, 79). In cultured cell lines, AMD-3100 did not significantly affect CXCL12/CXCR7 interactions at high concentrations, although AMD3100 did selectively block binding of CXCL12/CXCR4 (42). Furthermore, a recent study also suggests that AMD-3100 is a CXCR7 ligand with agonist properties when used at high concentrations (100–1,000 μM) (36). Thus AMD-3100 may have opposite effects on the two receptors, CXCR4 and CXCR7, depending on concentrations and context being evaluated (36, 79). In the current study, AMD-3100 was used below the concentration ranges documented to result in agonist effects mediated through the CXCR7 receptor, and it is clear that AMD-3100 is more effective at blocking binding of CXCL12/CXCR4 (42). However, studies evaluating the roles of CXCL12/CXCR4 and/or CXCL12/CXCR7 in the urinary bladder of control rats and those with urinary bladder inflammation are novel, not previously evaluated. Thus potential effects of CXCR7 receptor blockade cannot be ruled out, and it is a possibility that the overall changes in bladder function observed with AMD-3100 intravesical administration represent effects, perhaps opposite (36) or those involving cross talk (25) between CXCR4 and CXCR7. Future studies using high-affinity and selective CXCR7 ligands such as CCX771 (79) should be considered when defining the role of CXCR7 in bladder function.

To our knowledge, this is the first time the CXCR4 receptor antagonist AMD-3100 has been intravesically infused; thus, we needed to determine working dilutions empirically. Based on stromal cell adherence experiments, a concentration of 50

μM was attempted first in pilot studies (4). Whereas this concentration (50 μM) of AMD-3100 induced a similar increase in bladder capacity, an undesirable decrease in peak micturition pressure was also observed. Based on a concentration used in cultured epithelial cells (35), we then used 5 μM AMD-3100 and observed an increase in bladder capacity without changes in pressure; therefore, 5 μM AMD-3100 was used throughout the experiments in this study. This dose may not be optimal, since there is no literature precedent for intravesical instillation of AMD-3100. The effects on bladder function were observed in control and CYP-treated rats treated with this AMD-3100 dose; the effects were only observed on intercontraction interval and bladder capacity, not on bladder pressures. The absence of broad effects on all cystometric parameters suggests specificity in AMD-3100 action at the dose used in this study. Lack of effects on micturition pressures (i.e., baseline and peak micturition) in control and CYP-treated rats also suggests little or no effects on urethral outlet resistance.

Recently, the functional contribution of the urothelial lining of the urinary bladder has advanced beyond the view of the urothelium as a passive barrier to that of an active sensor with a potential signaling (i.e., sensory) role, especially in the context of urinary bladder inflammation (8). Urothelial cells share a number of similarities with sensory neurons, and the urothelium has been suggested (2, 8, 9, 61, 62, 63, 64) to have "neuronal-like" properties. Urothelial cells express numerous receptors similar to those found in DRG neurons such as purinergic, norepinephrine, acetylcholine, neuropeptide- and protease-activated receptors, acid sensing ion channels, neurotrophin receptors, and transient receptor potential channels (2, 8, 9, 61, 62, 63, 64). Therefore, it was not surprising to observe CXCL12/CXCR4 expression in the urothelium in control or CYP-treated rats given distribution of chemokines and associated receptors in DRG (6, 7, 33, 34, 49, 52, 60, 65, 67, 74, 80). The present study adds to the growing list of similarities between urothelial cells and sensory neurons.

In the present studies, we did not observe CXCL12 or CXCR4 immunostaining in the suburothelial plexus, and this was surprising, especially for CXCR4 given the numerous reports of CXCR4 expression in DRG cells (6, 7, 48, 49). Although we did not observe CXCL12/CXCR4 immunostaining in the suburothelial nerve plexus in whole mounts, urothelial cells (CXCL12 and CXCR4) and detrusor smooth muscle (CXCL12; data not shown) did exhibit immunostaining, so technical limitations such as antibody penetration do not seem plausible. Given the expression of CXCL12/CXCR4 in urothelial cells and detrusor smooth muscle but not in the suburothelial plexus, the mechanism(s) of action of CXCL12 likely excludes direct effects on the suburothelial nerve plexus. Urothelial cells secrete many signaling molecules in response to distention and exhibit altered secretion with bladder inflammation (2, 8, 9). Such signaling molecules include neurotrophins, neuropeptides, ATP, acetylcholine, prostanoids, nitric oxide (NO), and cytokines (2, 8, 9). Functional receptor expression coupled with chemical secretion capabilities enables the urothelium to respond to stimuli and reciprocally communicate with detrusor smooth muscle cells, suburothlelial nerve plexus, and/or interstitial cells (2, 8, 9). Therefore, it is possible that CXCL12 signaling via CXCR4 expression in urothelial cells may activate downstream targets that consequently facilitate the release of other mediators. Urothelial-derived mediators such as ATP or NO may then influence the suburothelial nerve plexus to affect micturition reflex function (2, 8, 9). Future studies assessing CXCL12-induced secretion of ATP and/or NO in urothelial cells and CXCL12-mediated effects on detrusor contractility in the presence and absence of urothelium are logical future directions to determine direct and indirect effects of CXCL12/CXCR4 signaling in micturition pathways.

Conclusions

These studies demonstrate a functional role for CXCL12/CXCR4 signaling in bladder function in normal rats and those with urinary bladder inflammation induced by CYP. Chemokines and associated receptor signaling may serve as potential targets for therapeutic intervention with respect to bladder inflammation.

ACKNOWLEDGMENTS

We acknowledge the technical expertise and support provided by the Vermont Cancer Center DNA Analysis Facility.

GRANTS

This work was funded by National Institutes of Health (NIH) grants DK-051369, DK-060481, and DK-065989. NIH Grant P20 RR-16435 from the Centers of Biomedical Research Excellence Program of the National Center also supported the project for Research Resources.

DISCLOSURES

No conflicts of interest are declared by the authors.

REFERENCES

1. **Abbadie C, Lindia JA, Cumiskey AM, Peterson LB, Mudgett JS, Bayne EK, DeMartino JA, MacIntyre DE, Forrest MJ.** Impaired neuropathic pain responses in mice lacking the chemokine receptor CCR2. *Proc Natl Acad Sci USA* 100: 7947–7952, 2003.
2. **Apodaca G, Balestreire E, Birder LA.** The uroepithelial-associated sensory web. *Kidney Int* 72: 1057–1064, 2007.
3. **Arms L, Vizzard MA.** Distribution and function of chemokine/receptor systems in cyclophosphamide (CYP)-induced cystitis in rats (Abstract). Program No. 372.19. 2009 Neuroscience Meeting Planner. Chicago, IL: Society for Neuroscience, 2009. Online.
4. **Azab AK, Runnels JM, Pitsillides C, Moreau AS, Azab F, Leleu X, Jia X, Wright R, Ospina B, Carlson AL, Alt C, Burwick N, Roccaro AM, Ngo HT, Farag M, Melhem MR, Sacco A, Munshi NC, Hideshima T, Rollins BJ, Anderson KC, Kung AL, Lin CP, Ghobrial IM.** CXCR4 inhibitor AMD3100 disrupts the interaction of multiple myeloma cells with the bone marrow microenvironment and enhances their sensitivity to therapy. *Blood* 113: 4341–4351, 2009.
5. **Balabanian K, Lagane B, Infantino S, Chow KY, Harriague J, Moepps B, Arenzana-Seisdedos F, Thelen M, Bachelerie F.** The chemokine SDF-1/CXCL12 binds to and signals through the orphan receptor RDC1 in T lymphocytes. *J Biol Chem* 280: 35760–35766, 2005.
6. **Bhangoo S, Ren D, Miller RJ, Henry KJ, Lineswala J, Hamdouchi C, Li B, Monahan PE, Chan DM, Ripsch MS, White FA.** Delayed functional expression of neuronal chemokine receptors following focal nerve demyelination in the rat: a mechanism for the development of chronic sensitization of peripheral nociceptors (Abstract). *Mol Pain* 3: 38, 2007.
7. **Bhangoo SK, Ren D, Miller RJ, Chan DM, Ripsch MS, Weiss C, McGinnis C, White FA.** CXCR4 chemokine receptor signaling mediates pain hypersensitivity in association with antiretroviral toxic neuropathy. *Brain Behav Immun* 21: 581–591, 2007.
8. **Birder LA.** Urinary bladder urothelium: molecular sensors of chemical/thermal/mechanical stimuli. *Vascul Pharmacol* 45: 221–226, 2006.
9. **Birder LA, de Groat WC.** Mechanisms of disease: involvement of the urothelium in bladder dysfunction. *Nat Clin Pract Urol* 4: 46–54, 2007.
10. **Birder LA, Nakamura Y, Kiss S, Nealen ML, Barrick S, Kanai AJ, Wang E, Ruiz G, De Groat WC, Apodaca G, Watkins S, Caterina MJ.**

Altered urinary bladder function in mice lacking the vanilloid receptor TRPV1. *Nat Neurosci* 5: 856–860, 2002.
11. **Birder LA, Wolf-Johnston A, Buffington CA, Roppolo JR, de Groat WC, Kanai AJ.** Altered inducible nitric oxide synthase expression and nitric oxide production in the bladder of cats with feline interstitial cystitis. *J Urol* 173: 625–629, 2005.
12. **Braas KM, May V, Zvara P, Nausch B, Kliment J, Dunleavy JD, Nelson MT, Vizzard MA.** Role for pituitary adenylate cyclase activating polypeptide in cystitis-induced plasticity of micturition reflexes. *Am J Physiol Regul Integr Comp Physiol* 290: R951–R962, 2006.
13. **Cheppudira BP, Girard BM, Malley SE, Dattilio A, Schutz KC, May V, Vizzard MA.** Involvement of JAK-STAT signaling/function after cyclophosphamide-induced bladder inflammation in female rats. *Am J Physiol Renal Physiol* 297: F1038–F1044, 2009.
14. **Cheppudira BP, Girard BM, Malley SE, Schutz KC, May V, Vizzard MA.** Upregulation of vascular endothelial growth factor isoform VEGF-164 and receptors (VEGFR-2, Npn-1, and Npn-2) in rats with cyclophosphamide-induced cystitis. *Am J Physiol Renal Physiol* 295: F826–F836, 2008.
15. **Chuang YC, Chancellor MB, Seki S, Yoshimura N, Tyagi P, Huang L, Lavelle JP, De Groat WC, Fraser MO.** Intravesical protamine sulfate and potassium chloride as a model for bladder hyperactivity. *Urology* 61: 664–670, 2003.
16. **Corrow KA, Vizzard MA.** Phosphorylation of extracellular signal-regulated kinases in urinary bladder in rats with cyclophosphamide-induced cystitis. *Am J Physiol Regul Integr Comp Physiol* 293: R125–R134, 2007.
17. **Dorr W.** Cystometry in mice–influence of bladder filling rate and circadian variations in bladder compliance. *J Urol* 148: 183–187, 1992.
18. **Driscoll A, Teichman JM.** How do patients with interstitial cystitis present? *J Urol* 166: 2118–2120, 2001.
19. **Erickson DR, Xie SX, Bhavanandan VP, Wheeler MA, Hurst RE, Demers LM, Kushner L, Keay SK.** A comparison of multiple urine markers for interstitial cystitis. *J Urol* 167: 2461–2469, 2002.
20. **Fitzgerald MP, Koch D, Senka J.** Visceral and cutaneous sensory testing in patients with painful bladder syndrome. *Neurourol Urodyn* 24: 627–632, 2005.
21. **Foster R, McClung C, Feldman P, Matthew R, Fitzgerald MP, White FA.** Pelvic floor muscle injury-induced tactile hypernoniceptive behavior is reversed by the administration of CXCR4 antagonist, AMD3100 (Abstract). Program No. 655.6. 2009 Neuroscience Meeting Planner. Chicago, IL: Society for Neuroscience, 2009. Online.
22. **Girard BM, May V, Bora SH, Fina F, Braas KM.** Regulation of neurotrophic peptide expression in sympathetic neurons: quantitative analysis using radioimmunoassay and real-time quantitative polymerase chain reaction. *Regul Pept* 109: 89–101, 2002.
23. **Gosselin RD, Dansereau MA, Pohl M, Kitabgi P, Beaudet N, Sarret P, Melik Parsadaniantz S.** Chemokine network in the nervous system: a new target for pain relief. *Curr Med Chem* 15: 2866–2875, 2008.
24. **Guerios SD, Wang ZY, Boldon K, Bushman W, Bjorling DE.** Blockade of NGF and trk receptors inhibits increased peripheral mechanical sensitivity accompanying cystitis in rats. *Am J Physiol Regul Integr Comp Physiol* 295: R111–R122, 2008.
25. **Hartmann TN, Grabovsky V, Pasvolsky R, Shulman Z, Buss EC, Spiegel A, Nagler A, Lapidot T, Thelen M, Alon R.** A crosstalk between intracellular CXCR7 and CXCR4 involved in rapid CXCL12-triggered integrin activation but not in chemokine-triggered motility of human T lymphocytes and CD34+ cells. *J Leukoc Biol* 84: 1130–1140, 2008.
26. **Hatse S, Princen K, Bridger G, De Clercq E, Schols D.** Chemokine receptor inhibition by AMD3100 is strictly confined to CXCR4. *FEBS Lett* 527: 255–262, 2002.
27. **Herrera GM, Pozo MJ, Zvara P, Petkov GV, Bond CT, Adelman JP, Nelson MT.** Urinary bladder instability induced by selective suppression of the murine small conductance calcium-activated potassium (SK3) channel. *J Physiol* 551: 893–903, 2003.
28. **Hu VY, Malley S, Dattilio A, Folsom JB, Zvara P, Vizzard MA.** COX-2 and prostanoid expression in micturition pathways after cyclophosphamide-induced cystitis in the rat. *Am J Physiol Regul Integr Comp Physiol* 284: R574–R585, 2003.
29. **Hu VY, Zvara P, Dattilio A, Redman TL, Allen SJ, Dawbarn D, Stroemer RP, Vizzard MA.** Decrease in bladder overactivity with REN1820 in rats with cyclophosphamide induced cystitis. *J Urol* 173: 1016–1021, 2005.
30. **Hurst RE, Moldwin RM, Mulholland SG.** Bladder defense molecules, urothelial differentiation, urinary biomarkers, and interstitial cystitis. *Urology* 69: 17–23, 2007.
31. **Jennings L, Vizzard MA.** Cyclophosphamide-induced inflammation of the urinary bladder alters electrical properties of small diameter afferent neurons from dorsal root ganglia (Abstracat). *FASEB J* 13: A57, 1999.
32. **Johansson S, Ogawa K, Fall M.** Interstitial cystitis. In: *The Pathology of Interstitial Cystitis*, edited by Sant GR. Philadelphia, PA: Lippincott-Raven, 1997, p. 143–152.
33. **Jung H, Bhangoo S, Banisadr G, Freitag C, Ren D, White FA, Miller RJ.** Visualization of chemokine receptor activation in transgenic mice reveals peripheral activation of CCR2 receptors in states of neuropathic pain. *J Neurosci* 29: 8051–8062, 2009.
34. **Jung H, Toth PT, White FA, Miller RJ.** Monocyte chemoattractant protein-1 functions as a neuromodulator in dorsal root ganglia neurons. *J Neurochem* 104: 254–263, 2008.
35. **Kajiyama H, Shibata K, Terauchi M, Ino K, Nawa A, Kikkawa F.** Involvement of SDF-1alpha/CXCR4 axis in the enhanced peritoneal metastasis of epithelial ovarian carcinoma. *Int J Cancer* 122: 91–99, 2008.
36. **Kalatskaya I, Berchiche YA, Gravel S, Limberg BJ, Rosenbaum JS, Heveker N.** AMD3100 is a CXCR7 ligand with allosteric agonist properties. *Mol Pharmacol* 75: 1240–1247, 2009.
37. **Klinger MB, Dattilio A, Vizzard MA.** Expression of cyclooxygenase-2 in urinary bladder in rats with cyclophosphamide-induced cystitis. *Am J Physiol Regul Integr Comp Physiol* 293: R677–R685, 2007.
38. **Klinger MB, Girard B, Vizzard MA.** p75NTR expression in rat urinary bladder sensory neurons and spinal cord with cyclophosphamide-induced cystitis. *J Comp Neurol* 507: 1379–1392, 2008.
39. **Klinger MB, Vizzard MA.** Role of p75NTR in female rat urinary bladder with cyclophosphamide-induced cystitis. *Am J Physiol Renal Physiol* 295: F1778–F1789, 2008.
40. **Lamale LM, Lutgendorf SK, Zimmerman MB, Kreder KJ.** Interleukin-6, histamine, and methylhistamine as diagnostic markers for interstitial cystitis. *Urology* 68: 702–706, 2006.
41. **Lindia JA, McGowan E, Jochnowitz N, Abbadie C.** Induction of CX3CL1 expression in astrocytes and CX3CR1 in microglia in the spinal cord of a rat model of neuropathic pain. *J Pain* 6: 434–438, 2005.
42. **Luker K, Gupta M, Luker G.** Bioluminescent CXCL12 fusion protein for cellular studies of CXCR4 and CXCR7. *Biotechniques* 47: 625–632, 2009.
43. **Malley SE, Vizzard MA.** Changes in urinary bladder cytokine mRNA and protein after cyclophosphamide-induced cystitis. *Physiol Genomics* 9: 5–13, 2002.
44. **Matthys P, Hatse S, Vermeire K, Wuyts A, Bridger G, Henson GW, De Clercq E, Billiau A, Schols D.** AMD3100, a potent and specific antagonist of the stromal cell-derived factor-1 chemokine receptor CXCR4, inhibits autoimmune joint inflammation in IFN-gamma receptor-deficient mice. *J Immunol* 167: 4686–4692, 2001.
45. **Mikami S, Nakase H, Yamamoto S, Takeda Y, Yoshino T, Kasahara K, Ueno S, Uza N, Oishi S, Fuji N, Nagasawa T, Chiba T.** Blockade of CXCL12/CXCR4 axis ameliorates murine experimental colitis. *J Pharmacol Exp Ther* 327: 383–392, 2008.
46. **Milligan ED, Zapata V, Chacur M, Schoeniger D, Biedenkapp J, O'Connor KA, Verge GM, Chapman G, Green P, Foster AC, Naeve GS, Maier SF, Watkins LR.** Evidence that exogenous and endogenous fractalkine can induce spinal nociceptive facilitation in rats. *Eur J Neurosci* 20: 2294–2302, 2004.
47. **Nazif O, Teichman JM, Gebhart GF.** Neural upregulation in interstitial cystitis. *Urology* 69: 24–33, 2007.
48. **Oh SB, Endoh T, Simen AA, Ren D, Miller RJ.** Regulation of calcium currents by chemokines and their receptors. *J Neuroimmunol* 123: 66–75, 2002.
49. **Oh SB, Tran PB, Gillard SE, Hurley RW, Hammond DL, Miller RJ.** Chemokines and glycoprotein120 produce pain hypersensitivity by directly exciting primary nociceptive neurons. *J Neurosci* 21: 5027–5035, 2001.
50. **Parsons CL.** The role of the urinary epithelium in the pathogenesis of interstitial cystitis/prostatitis/urethritis. *Urology* 69: 9–16, 2007.
51. **Petrone R, Agha A, Roy J, Hurst R.** Urodynamic findings in patients with interstitial cystitis (Abstract). *J Urol* 153: 290A, 1995.
52. **Qin X, Wan Y, Wang X.** CCL2 and CXCL1 trigger calcitonin gene-related peptide release by exciting primary nociceptive neurons. *J Neurosci Res* 82: 51–62, 2005.

53. **Rutkowski MD, DeLeo JA.** The Role of Cytokines in the Initiation and Maintenance of Chronic Pain. *Drug News Perspect* 15: 626–632, 2002.
54. **Sakthivel SK, Singh UP, Singh S, Taub DD, Novakovic KR, Lillard JW Jr.** CXCL10 blockade protects mice from cyclophosphamide-induced cystitis (Abstract). *J Immune Based Ther Vaccines* 6: 6, 2008.
55. **Sant GR, Hanno PM.** Interstitial cystitis: current issues and controversies in diagnosis. *Urology* 57: 82–88, 2001.
56. **Sant GR, Kempuraj D, Marchand JE, Theoharides TC.** The mast cell in interstitial cystitis: role in pathophysiology and pathogenesis. *Urology* 69: 34–40, 2007.
57. **Savarin-Vuaillat C, Ransohoff RM.** Chemokines and chemokine receptors in neurological disease: raise, retain, or reduce? *Neurotherapeutics* 4: 590–601, 2007.
58. **Sengupta S, Schiff R, Katzenellenbogen BS.** Post-transcriptional regulation of chemokine receptor CXCR4 by estrogen in HER2 overexpressing, estrogen receptor-positive breast cancer cells. *Breast Cancer Res Treat* 117: 243–251, 2009.
59. **Studeny S, Cheppudira BP, Meyers S, Balestreire EM, Apodaca G, Birder LA, Braas KM, Waschek JA, May V, Vizzard MA.** Urinary Bladder Function and Somatic Sensitivity in Vasoactive Intestinal Polypeptide (VIP)(−/−) Mice. *J Mol Neurosci* 36: 175–187, 2008.
60. **Sun JH, Yang B, Donnelly DF, Ma C, LaMotte RH.** MCP-1 enhances excitability of nociceptive neurons in chronically compressed dorsal root ganglia. *J Neurophysiol* 96: 2189–2199, 2006.
61. **Sun Y, Chai TC.** Augmented extracellular ATP signaling in bladder urothelial cells from patients with interstitial cystitis. *Am J Physiol Cell Physiol* 290: C27–C34, 2006.
62. **Sun Y, Chai TC.** Up-regulation of P2X3 receptor during stretch of bladder urothelial cells from patients with interstitial cystitis. *J Urol* 171: 448–452, 2004.
63. **Sun Y, Keay S, De Deyne PG, Chai TC.** Augmented stretch activated adenosine triphosphate release from bladder uroepithelial cells in patients with interstitial cystitis. *J Urol* 166: 1951–1956, 2001.
64. **Sun Y, Keay S, Lehrfeld TJ, Chai TC.** Changes in adenosine triphosphate-stimulated ATP release suggest association between cytokine and purinergic signaling in bladder urothelial cells. *Urology* 74: 1163–1168, 2009.
65. **Tanaka T, Minami M, Nakagawa T, Satoh M.** Enhanced production of monocyte chemoattractant protein-1 in the dorsal root ganglia in a rat model of neuropathic pain: possible involvement in the development of neuropathic pain. *Neurosci Res* 48: 463–469, 2004.
66. **Vera PL, Iczkowski KA, Wang X, Meyer-Siegler KL.** Cyclophosphamide-induced cystitis increases bladder CXCR4 expression and CXCR4-macrophage migration inhibitory factor association. *PLoS ONE* 3: e3898, 2008.
67. **Verge GM, Milligan ED, Maier SF, Watkins LR, Naeve GS, Foster AC.** Fractalkine (CX3CL1) and fractalkine receptor (CX3CR1) distribution in spinal cord and dorsal root ganglia under basal and neuropathic pain conditions. *Eur J Neurosci* 20: 1150–1160, 2004.
68. **Vizzard MA.** Alterations in neuropeptide expression in lumbosacral bladder pathways following chronic cystitis. *J Chem Neuroanat* 21: 125–138, 2001.
69. **Vizzard MA.** Alterations in spinal cord Fos protein expression induced by bladder stimulation following cystitis. *Am J Physiol Regul Integr Comp Physiol* 278: R1027–R1039, 2000.
70. **Vizzard MA.** Changes in urinary bladder neurotrophic factor mRNA and NGF protein following urinary bladder dysfunction. *Exp Neurol* 161: 273–284, 2000.
71. **Vizzard MA.** Up-regulation of pituitary adenylate cyclase-activating polypeptide in urinary bladder pathways after chronic cystitis. *J Comp Neurol* 420: 335–348, 2000.
72. **Vizzard MA, Boyle MM.** Increased expression of growth-associated protein (GAP-43) in lower urinary tract pathways following cyclophosphamide (CYP)-induced cystitis. *Brain Res* 844: 174–187, 1999.
73. **White FA, Jung H, Miller RJ.** Chemokines and the pathophysiology of neuropathic pain. *Proc Natl Acad Sci USA* 104: 20151–20158, 2007.
74. **White FA, Sun J, Waters SM, Ma C, Ren D, Ripsch M, Steflik J, Cortright DN, Lamotte RH, Miller RJ.** Excitatory monocyte chemoattractant protein-1 signaling is up-regulated in sensory neurons after chronic compression of the dorsal root ganglion. *Proc Natl Acad Sci USA* 102: 14092–14097, 2005.
75. **Wu XR, Kong XP, Pellicer A, Kreibich G, Sun TT.** Uroplakins in urothelial biology, function, and disease. *Kidney Int* 75: 1153–1165, 2009.
76. **Yoshimura N, Bennett NE, Hayashi Y, Ogawa T, Nishizawa O, Chancellor MB, de Groat WC, Seki S.** Bladder overactivity and hyperexcitability of bladder afferent neurons after intrathecal delivery of nerve growth factor in rats. *J Neurosci* 26: 10847–10855, 2006.
77. **Yoshimura N, de Groat WC.** Increased excitability of afferent neurons innervating rat urinary bladder after chronic bladder inflammation. *J Neurosci* 19: 4644–4653, 1999.
78. **Yuridullah R, Corrow KA, Malley SE, Vizzard MA.** Expression of fractalkine and fractalkine receptor in urinary bladder after cyclophosphamide (CYP)-induced cystitis. *Auton Neurosci* 126–127: 380–389, 2006.
79. **Zabel BA, Wang Y, Lewen S, Berahovich RD, Penfold ME, Zhang P, Powers J, Summers BC, Miao Z, Zhao B, Jalili A, Janowska-Wieczorek A, Jaen JC, Schall TJ.** Elucidation of CXCR7-mediated signaling events and inhibition of CXCR4-mediated tumor cell transendothelial migration by CXCR7 ligands. *J Immunol* 183: 3204–3211, 2009.
80. **Zhang N, Inan S, Cowan A, Sun R, Wang JM, Rogers TJ, Caterina M, Oppenheim JJ.** A proinflammatory chemokine, CCL3, sensitizes the heat- and capsaicin-gated ion channel TRPV1. *Proc Natl Acad Sci USA* 102: 4536–4541, 2005.
81. **Zhang Z, Zhong W, Hall MJ, Kurre P, Spencer D, Skinner A, O'Neill S, Xia Z, Rosenbaum JT.** CXCR4 but not CXCR7 is mainly implicated in ocular leukocyte trafficking during ovalbumin-induced acute uveitis. *Exp Eye Res* 89: 522–531, 2009.
82. **Zvara P, Vizzard MA.** Exogenous overexpression of nerve growth factor in the urinary bladder produces bladder overactivity and altered micturition circuitry in the lumbosacral spinal cord (Abstract). *BMC Physiol* 7: 9, 2007.
83. **Zvarova K, Vizzard MA.** Changes in galanin immunoreactivity in rat micturition reflex pathways after cyclophosphamide-induced cystitis. *Cell Tissue Res* 324: 213–224, 2006.